Romanian Reports in Physics **74**, 707 (2022)

SEISMIC MOMENT TENSOR SOLUTIONS FOR GEOPHYSICAL MAPPING OF THE PHILIPPINE SEA BASIN BY GMT

POLINA LEMENKOVA

Université Libre de Bruxelles, École Polytechnique de Bruxelles (EPB, Brussels Faculty of Engineering), Laboratory of Image Synthesis and Analysis. Building L, Campus de Solbosch CP131/3, Avenue Franklin D. Roosevelt 50, B-1050 Brussels, Belgium
ORCID ID: https://orcid.org/0000-0002-5759-1089
Email: *polina.lemenkova@ulb.be*

Received April 23, 2022

Abstract. This paper presents a GMT scripting technique for mapping seismic moment tensor solutions. The underlying geophysical properties and settings of the Philippine Sea Plate (PSP) situated on the margins of the Pacific Ocean are analysed. Active volcanism and high seismicity of this region located along the margins of the Philippine Sea Basin (PSB) results in a series of earthquake events caused by geodynamic processes of tectonic plate subduction. The proposed console-based framework of cartographic workflow is designed to perform mapping of the earthquake events using Generic Mapping Tools (GMT) modules, to analyse seismic setting through visualisation of the geophysical dataset. The materials include General Bathymetric Chart of the Oceans (GEBCO), Centroid Moment Tensor (CMT) and International Seismological Centre (ISC) seismic data. Technically, the algorithm of mapping by GMT consists in a consecutive use of modules used in a script run from a command line: 'psmeca', 'psvelo', 'img2grd', 'grdtrack', 'grdimage'. The GMT functionality is illustrated by the key snippets of code. The path to the full codes is provided with a link to the author's GitHub repository for technical repeatability. Furthermore, the algorithm of GMT enabled to visualise CMT solutions for shallow depth earthquakes of $Mw < 10$ along the PSB margins from 1976 to 2010. Thus, the paper also demonstrated and presented the performance of the GMT on a geophysical dataset that features complete earthquakes data along the zone of tectonic plate subduction from the Global CMT Project. In both technical and geophysical cases, this approach of GMT-based mapping presents cartographic workflow better than state-of-the-art traditional GIS programs through increased automation of the cartographic workflow. The study contributed to the development of methods of geophysical and seismic mapping using GMT scripting toolset by visualising focal mechanisms and seismic moment tensor solutions.

Key words: Earthquake, seismicity, cartography, shell script, Pacific Ocean.

1. INTRODUCTION

1.1. BACKGROUND

This paper addresses the problem of cartographic data handling for geophysical mapping. The study area includes seismically active region of the seafloor located

on the borders of the tectonic plates in the PSB located in the west Pacific Ocean. Subducting lithosphere plates activate complex processes along their margins that results in complex seismic activities in the upper mantle and associated repetitive submarine earthquakes [12, 36, 45, 63]. Mapping such tectonically unstable regions is critical for analysis of the seismicity, as it helps highlighting the relationship among earthquake location and complexity of the marine geophysical processes [18, 52, 58, 68]. A lack of knowledge of the topography of the seabed restricts the progress of geophysical investigations of the oceans as well as geological exploration and exploiting mineral resources which might be found in the bed of the ocean [11]. This rises a question of developing advanced methods of geophysical mapping.

Advances in programming made an application of scripting in cartographic mapping become real: using programming codes for generating maps from a console in a semi-automated regime [10, 42, 49]. Using scripting techniques is beneficial for geophysical studies from rapid and accurate data processing. For instance, in the analysis of large seismic datasets with complex multi-column tables, the capability of machine-based executing script is highly desirable for quick data visualisation and analysis [37, 50, 56]. Specifically for marine geophysics, it is necessary to use the advanced cartographic tools that can be used for mapping seismic data in advance of any potential risk of geologic activities and help preventing natural hazards, such as earthquakes and tsunamis [47, 53].

Although seismic mapping and prediction of geophysical hazards is quite an important problem in studies of physics of the Earth, using cartographic scripting techniques remains a novel method for the domain of marine geophysics where state-of-the-art software such as GIS is traditionally used. This work proposes a scripting cartographic framework based on using the GMT, which has a modular structure enabling cartographic elements to be plotted from the console. In order to enable the repeatability of the methods and to test the efficacy of the workflow, the most important fragments of scripts are presented with the full access to the codes provided using the GitHub repository of the author.

Specifically, this paper proposes a novel approach for accurate and rapid cartographic visualisation of the geophysical data aimed at visualising seismic parameters reflecting complex geophysical activities in the west region of the Pacific Ocean: the PSB. Advanced cartographic visualisation helps discovering the casual relationships between constituent geophysical and geological processes reflected in predicted seismic characteristics in the given region of the seafloor. The key of the scripting approach in cartography is to utilise the modules of GMT for plotting cartographic units, structures and elements on the map. It is thus possible to make the use of modules for automated mapping through the templates for subsequent maps in a series, which optimises mapping workflow through automation.

Active use of the machine-based cartographic data processing provides an ef-

fective tool for real-time mapping, which is crucial for geophysical mapping. It is especially actual for mapping high seismicity regions where accurate and rapid data visualisation is needed for prognosis and operative preventing of seismic risks. The script-based mapping of geophysical data was performed using the materials obtained from the open sources, such as GEBCO, CMT and ISC seismic data. The use of GMT achieved superior performance for geophysical mapping and improved the workflow of the cartographic techniques.

1.2. RELATED WORK

Earlier studies on the marine geophysical mapping highlighted right relationship between the geomorphic patterns of the deep-sea channels, submarine fans and their topography related to the mid-ocean ridge tectonics, volcanism and dynamics of the Philippine back arc [4, 14, 24, 31, 38], as well as earthquakes and gravitation [30]. Double seismic zone beneath the Mariana Island arc is well explained by the conceptual scheme of the processes of the global plate tectonics [43]. Thus, subduction of the cooled plate into the mantle causes formation of the deep ocean trenches where earthquakes and tsunamis originate as a consequence of high seismicity.

Regional geomorphology of the seafloor is formed under certain geologic-geophysical interactions affected by the influence of particular tectonic and geodynamic processes. Thus, the geomorphological evolution of the seafloor is largely controlled by geological evolution and tectonic plate dynamics [15, 17, 35, 41], geophysical processes [23, 34, 60], submarine volcanism and seismicity, see [22, 39, 51]. Mapping geological structure and visualising geophysical setting is a basic methodology for recognition of complex geophysical activities on the seafloor of the Pacific Ocean [19, 26, 46]. These studies extend the types and strength of geological processes, including seismicity, that can be better understood by mapping.

Active volcanism around Philippine Sea margins (Fig. 7) shows earthquake events demonstrating high seismicity of the region caused by tectonic plates subduction. Thus, subducting lithospheric plate acts as a giant radiator of the heat cooling, thickening, and progressively subsiding from ridge to trench. As a result, spreading seafloor, affected by moving plates, creates an axial rift, corrugated hills and ridges formed by the nearby faults. Moreover, plate subduction activates such processes as trench roll-back, arc rupture and back-arc rifting of the two interconnected back-arc basins: the Parece Vela and the Shikoku Basins. The Kyushu-Palau Ridge (KPR), a remnant arc of the active Izu-Bonin-Mariana trench (IBM) system results from the spreading of the Shikoku Basin (Fig. 1).

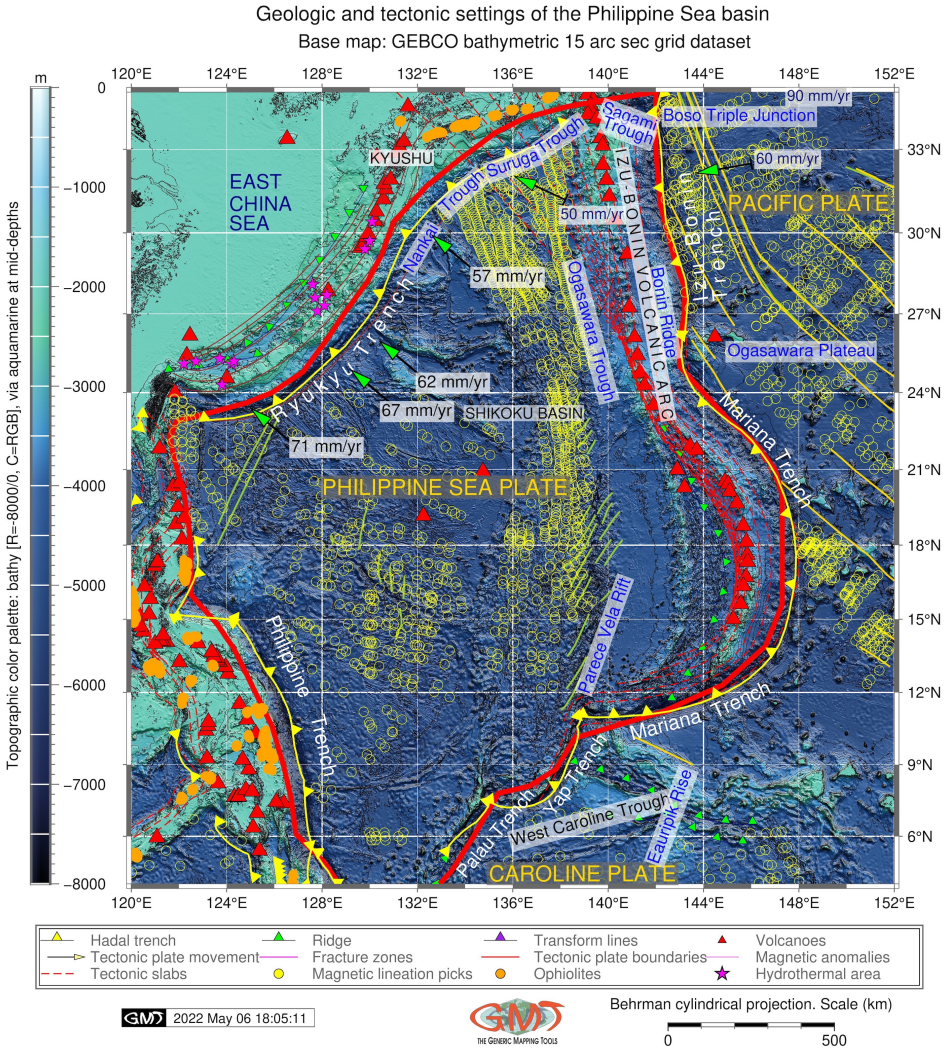

Fig. 1 – (Color online) Geologic map of the PSB. Solid red lines indicate boundaries between the lithospheric plates. Yellow fronts denote trench axes. Tectonic slab contours are depicted by the red dashed lines. Green arrows and relevant numbers indicate the convergence rates (mm/year) along the trenches. Magenta triangles denote hydrothermal areas mostly located along the Ryukyu Trench. Source: author.

In such a way, it plays a key role in the subduction process of the west PSP: the subduction zone here is characterised by the subducting beneath the Kyushu Arc, Fig. 1 [3]. A set of geodynamic processes including subduction-interface rheology, phase-transition buoyancy, slab stagnation, rollback of mantle and ridge-push

effects, cause significant trench motion of the IBM detected as advance by global plate-motion observations [2, 5].

2. MATERIALS AND METHODS

2.1. SEISMIC MAPPING

Current paper presents a report on the GMT cartographic techniques applied for geophysical mapping. Focal mechanisms (Fig. 3) were drawn using the 'psmeca' module of GMT that reads dataset values from the American Standard Code for Information Interchange (ASCII) file and generates a PostScript code plotting focal mechanisms. The full codes used for mapping in this study are available in the GitHub repository of the author in open access for repeatability in similar studies: https://github.com/paulinelemenkova/Mapping_seismic_moment_tensor_solutions

Focal mechanisms depict a commonly accepted theory of the focal depths of the earthquake showing a depth from the surface to the earthquake's origin (hypocenter). A dataset used in this study contains a significant amount of shallow earthquakes of the PSB with focal depths of several tens km (mostly < 50), intermediate earthquakes with focal depths from 70 to 200 km, and also a few earthquakes of the PSB with a deep focus reaching depths > 500 km, Table 2. The foci of the most PSB earthquakes are concentrated in the crust and upper mantle, *i.e*, originate in the shallow parts of the Earth's interior.

Table 1 Earthquake events for 1976/1977

Location code	Date	Centroid Time	Lat (°N)	Lon (°E)	Depth	HD*	CHT**
021576A PHILIPPINE ISL	1976/2/15	1:54:30.3 GMT	13.12	126.02	15.6	4.2	7.2
060776A LUZON PHILIPPINE ISL	1976/6/7	7:36:0.3 GMT	14.23	125.07	24.4	4.8	4.9
081676B LEYTE	1976/8/16	16:11:58.7 GMT	7.07	123.75	33.0	21.7	51.4
081776A LEYTE PHILIPPINE ISL	1976/ 8/17	1:11:16.5 GMT	10.08	126.10	47.3	2.6	6.3
081776B MINDANAO	1976/8/17	4:19:39.8 GMT	7.14	123.01	15.0	8.7	12.5
092976A MINDANAO	1976/9/29	21: 2:31.5 GMT	6.61	124.24	15.0	1.8	-1.2
110776B MINDANAO	1976/11/7	17: 9:13.7 GMT	8.35	126.86	42.1	6.2	7.6
112276A MINDANAO	1976/11/22	4:22:20.7 GMT	7.03	123.58	60.0	3.0	-4.6
121476A RYUKYU ISLANDS	1976/12/14	16: 6:49.2 GMT	28.12	130.64	15.0	3.8	4.8
010177C SOUTH OF HONSHU JAPAN	1977/ 1/1	11:33:45.9 GMT	30.62	136.80	476.5	1.8	4.3
010777B TAIWAN REGION	1977/1/7	19:36:48.6 GMT	20.78	120.01	10.0	2.5	1.7
010877A LUZON PHILIPPINE IS.	1977/1/8	6:41:10.9 GMT	15.77	122.73	13.3	1.6	6.8
011577A PHILIPPINE ISL	1977/1/15	10:49: 8.8 GMT	12.80	126.06	32.9	2.2	3.0
011777A BONIN ISL REGION	1977/1/17	6:23:40.7 GMT	26.40	142.74	13.9	3.4	4.6
011977B MINDANAO	1977/1/19	13:54: 9.8 GMT	5.01	126.56	50.1	4.8	5.3
012077A MINDANAO, PHILIPPINE	1977/1/20	20:51:17.2 GMT	8.00	122.70	41.8	2.3	2.3
022777A MARIANA ISLANDS	1977/ 2/27	18:34:15.0 GMT	18.21	145.30	592.6	2.1	6.5
022877B MINDANAO, PHILIPPINE IS	1977/2/28	1:50:38.7 GMT	8.87	127.01	55.8	2.3	6.8
030277B MINDANAO, PHILIPPINE IS	1977/3/2	9:53:26.4 GMT	6.62	123.53	33.4	6.0	3.2

*Half duration; **Centroid hypocenter time (HT)

Fig. 2 – Earthquake events for 1976/1977.

The original dataset of the focal mechanism solutions are from the was taken from the Global CMT Catalog, formerly known as the Harvard CMT catalog [8].

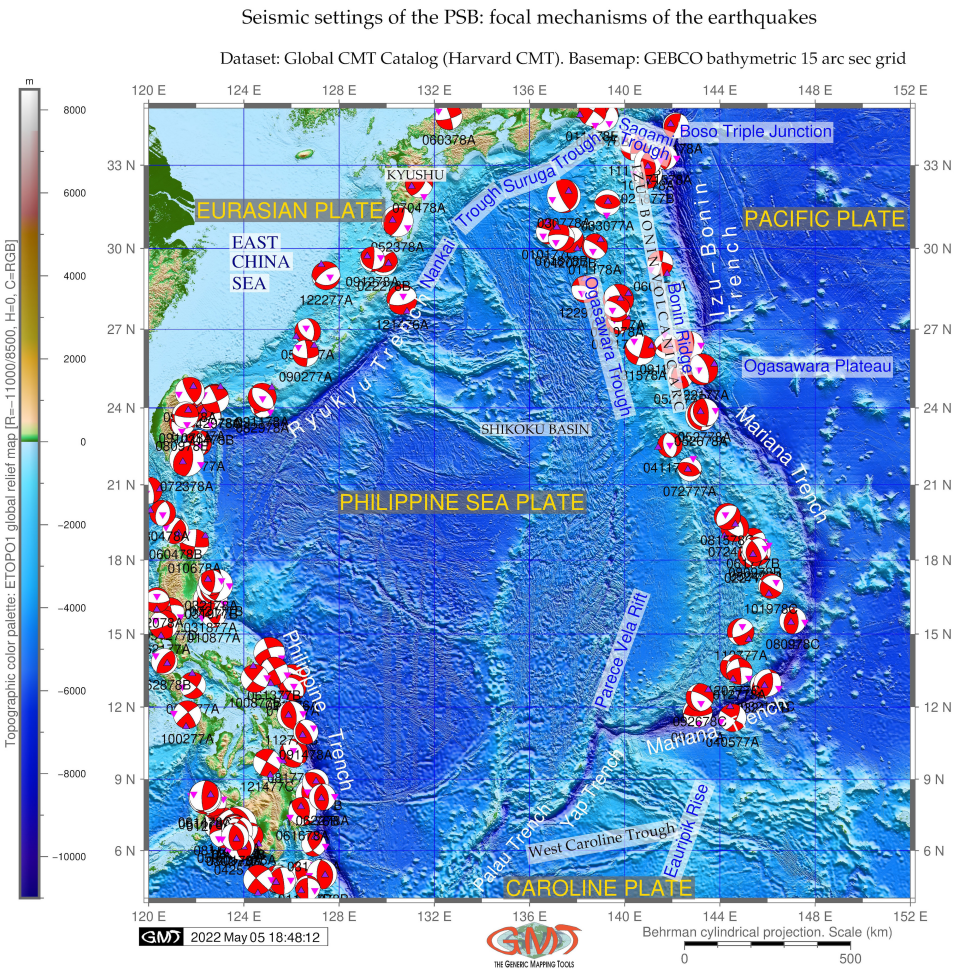

Fig. 3 – Seismic map of the focal mechanisms: PSB margins. The centroid moment tensor solutions for shallow depth earthquakes of $Mw < 10$ along the PSB margins, 1976 to 2010. Earthquakes along the tectonic plate subduction zone are shown by GMT. Data: Global CMT Project. Source: author.

Technical parameters are set up as following:

1. Moment magnitude (Mw) < 10;
2. Surface wave magnitude (Ms): < 10;
3. Body wave magnitude (Mb): < 10;
4. Data time span: 1976-2010.

While magnitude is a widely understood concept, describing the energy of the earthquake release on a logarithmic scale, some technical details are presented in

Figs. 2 and 4 used for mapping velocity (Fig. 6), assigning and interpreting magnitudes. Introduced in the 1930's, the Richter Scale (RS) is the best known scale for measuring the magnitude of earthquakes [33]. The Surface wave magnitude (Ms), creating the strongest disturbance within the upper layers of the Earth, is computed by the following algebraic formula: $MS = log10(A/T) + 1.66log10(D) + 3.30$, where T is the measured wave period and D is the distance in radians.

Table 2 Magnitude and Moment Tensor

Location code	Moment Tensor	Mw*	Mb**	Ms***	SM****	FP_1*****	FP_2******
021576A Philippine Isl	Expo=25 -5.140 3.270 1.860 -1.560 0.510 -4.690	6.5	6.1	6.1	$6.47e+25$	322/39/-73	121/53/-104
060776A Luzon	Expo=25 -0.930 5.570 -4.630 -1.810 2.820 -5.740	6.5	6.1	6.4	8.35e+25	249/67/180	339/90/23
081676B Mindanao	Expo=27 9.330 0.240 -9.570 1.450 -3.340 4.330	8.0	6.4	7.9	1.09e+28	341/35/92	158/55/-89
081776A Leyte Philippines	Expo=25 -1.250 0.390 0.860 -0.500 0.070 -0.570	6.0	6.0	5.7	1.34e+25	340/39/67	131/55/-108
081776B Mindanao	Expo=26 -1.220 5.310 -4.100 -1.920 1.330 2.110	7.1	6.2	6.8	5.71e+26	214/64/-172	120/83/-26
081776B Mindanao	Expo=24 -4.620 2.220 2.400 -0.530 -1.810 1.870	5.7	6.0	5.4	4.78e+24	232/35/-76	34/56/-100
110776B Mindanao	Expo=26 1.540 0.230 -1.770 0.990 0.610 -0.170	6.8	6.0	6.8	2.03e+26	162/39/49	30/62/118
112276A Mindanao	Expo=23 2.030 4.260 -6.290 1.780 2.020 0.220	5.1	6.0	0.0	6.07e+23	136/59/14	38/78/148
121476A Ryukyu Isl	Expo=25 -4.160 2.940 1.230 -2.490 0.330 1.350	6.4	6.3	6.2	4.62e+25	230/33/-114	78/61/-75
010177C Honshu Japan	Expo=24 -0.324 0.799 -0.475 1.014 -0.356 0.401	5.4	5.2	0.0	1.34e+24	33/32/-163	289/81/-59
010777B Taiwan Region	Expo=24 -3.009 -0.044 3.054 1.185 -2.128 -0.023	5.7	5.7	5.1	3.88e+24	194/29/-62	343/65/-105
010877A Luzon Philippines	Expo=23 6.364 2.443 -8.807 1.626 -1.176 2.219	5.2	5.3	0.0	8.16e+23	8/43/118	152/53/67
011577A Philippine Isl Reg	Expo=24 -1.842 1.248 0.594 -0.737 0.570 -1.652	5.5	5.6	4.6	2.41e+24	311/34/-88	128/56/-91
011777A Bonin Isl Reg	Expo=24 4.813 0.539 -5.352 0.757 4.521 0.467	5.8	5.6	5.6	6.87e+24	164/25/71	5/66/99
011977B Mindanao	Expo=25 1.646 -0.866 -0.781 -0.990 0.267 1.834	6.2	5.8	5.9	2.45e+25	161/40/130	293/61/62
012077A Mindanao	Expo=24 0.044 1.453 -1.496 0.517 0.947 1.691	5.5	5.4	4.9	2.49e+24	111/65/3	20/87/155
022777A Mariana Islands	Expo=24 -1.502 -0.378 1.880 -0.671 -0.473 -0.742	5.5	5.0	0.0	2.04e+24	136/48/-132	10/56/-53
022877B Mindanao	Expo=24 2.750 -1.458 -1.292 0.444 -0.274 0.678	5.5	5.7	0.0	2.46e+24	313/39/92	130/51/88
030277B Mindanao	Expo=25 3.195 -3.570 0.375 0.728 -1.526 2.261	6.4	6.1	6.1	4.34e+25	271/41/53	135/58/117

*Moment magnitude (Mw); ** Body wave magnitude (Mb); ***Surface wave magnitude (Ms); ****SM: Scalar Moment; *****Fault Plane (FP); ******strike/dip/slip.

Fig. 4 – Magnitude and Moment Tensor for the region of the Philippine Sea basin.

In contrast, deep earthquakes do not generate large surface waves. Therefore, the Body wave magnitude (Mb) is scaled based on the seismic waves penetrating through the Earth's interior (body) [33]. The Mb is measured based on the maximum amplitude A by formula: $Mb = log10(A/T) + Q(D,h)$, where T is the wave period and Q is an empirical function of focal depth h and epicentral distance D.

The Moment magnitude (Mw) relies on an underlying robust physical and mathematical development through converting seismic moment using a formula calibrated to agree with the Ms over much of its range. Others parameters are taken as the default ones. The data are collected in both GMT 'psvelomeca' and GMT 'psmeca' input formats and examined. Final solution was for GMT 'psmeca' (the reason is

for the GMT version 5.4.5 compatibility). The focal mechanisms are derived from a solution of the earthquakes' moment tensor, which is estimated by an analysis of the observed seismic waveforms.

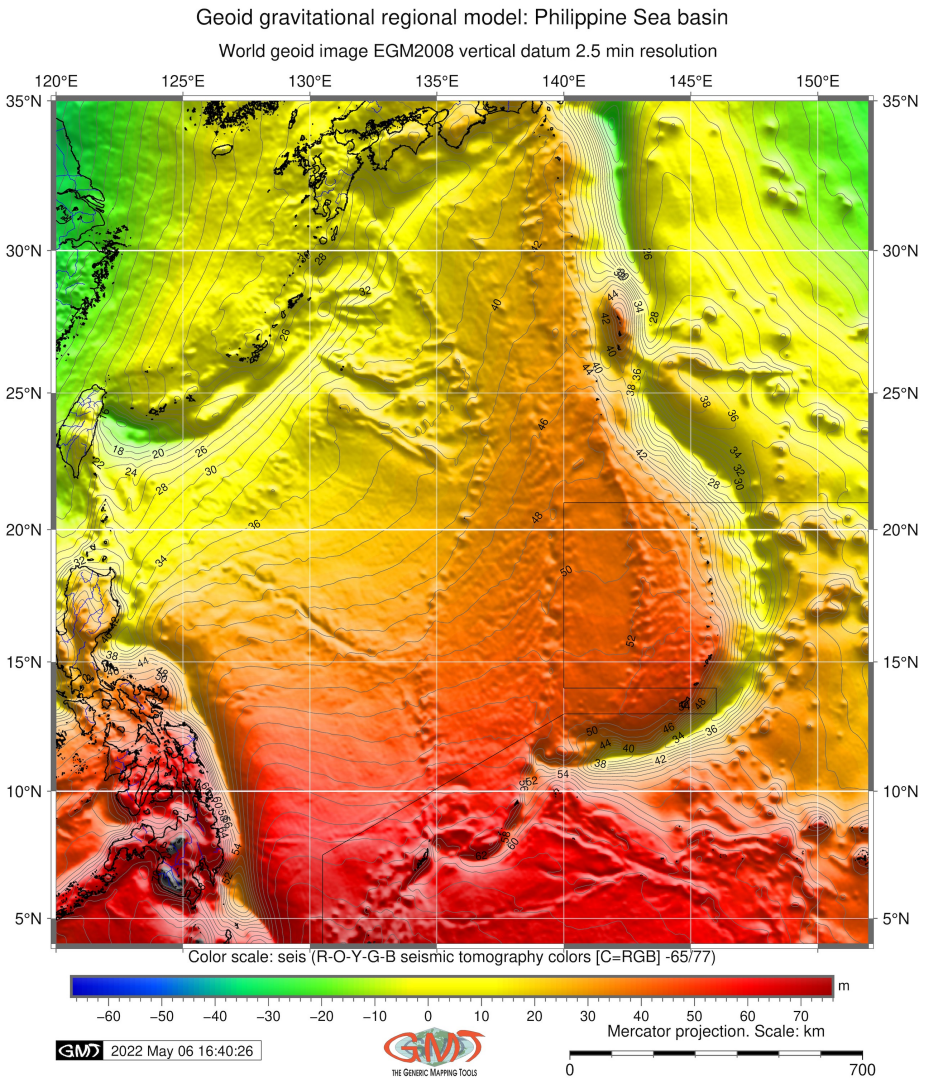

Fig. 5 – Geoid model based on Earth Gravitational Model 2008 grid at PSB margins. Data: [40]. Mapping: GMT. Source: author.

Technically, the seismic moment tensor (Harvard CMT, with zero trace) was plotted (Fig. 3) by 'psmeca' module using the following GMT code snippet:

$gmtpsmeca - RCMT.txt - J - Sd0.5/8/u - Gred - L0.1p - Fa/5p/it$
$- Fepurple - Fgmagenta - Ft - W0.1p - Fz - Ewhite - O - K >> \$ps.$

The scale (0.5) was adjusted to the scaling of the 'beach ball' radius, which is proportional to the magnitude. Here the '-Sd0.5/8/u' implies the scale, label size and annotation placement below the 'beach ball'. Filling the extensive quadrants was defined by -E parameter; -L parameter defines drawing the 'beach ball' outline of 0.1 pt. Shaded compressional quadrants of the focal mechanism 'beach ball' are colored by -Gred function. The -Fa/5p/it option was used to plot size, P_axis_symbol and T_axis_symbol, to compute and plot P and T axes with symbols (here: selected inverse triangle (i) and triangle (t), respectively).

The focal mechanisms (Fig. 3), visualised as commonly accepted in geophysical mapping 'beachballs', show a representation of the lower half of the focal sphere as viewed from above the focus at the earthquake epicenter and respective zones of compression and dilatation. Based on the recorded P-waves dataset, a graphical model shows red areas of the 'beachballs' as an upward moving, *i.e.*, the compressional motion, while white areas – a downward, dilatational motion. Determining the geological information, such as the rupture of the Earth's surface, it depicts the two nodal planes, a fault and an auxiliary one. For instance, the auxiliary plane intersects the line of the fault plane between the circle and its centre of the 'beachball' with a general rule that the closer the intersection to the centre is, the more dominant is the strike slip. The increase of the curvature of the crossing hemispheres denotes a shallower dip.

The strike of a nodal plane is measured in the degrees around the circle from the north to the line of the nodal plane. Based on the existing classification [33], various focal plane solutions are shown as follows:

- normal fault striking north, dipping E/W at ca. 45°
- oblique fault, right or left lateral and reverse slip
- oblique fault, reverse slip dominant, with some right/left lateral
- oblique fault, strike slip dominant, attitude ca. N° 40W / 70° W (right/left lateral), or N35° E / 70° E (left/right lateral)

The geoid model was plotted based on the Earth Gravitational Model 1996 (EGM96) grid at PSB margins using the geophysical data [40], GMT, Fig. 5. The earthquakes event map at PSB area (Fig. 7) shows the prime hypocentres and magnitude values by colour and size of the circles, respectively. The map was plotted on the basis of ISC-Engdahl-van der Hilst-Buland algorithm (EHB) Bulletin and overplayed on the Google Earth map as a file in a Keyhole Markup language Zipped (KMZ) format, which is an extension for a placemark file used by the Google Earth. The geographic coordinates include the x, y, z components in decimal degrees defined by the World Geodetic System 1984 (WGS84), Fig. 7.

2.2. VELOCITY MAPPING

The velocity ellipses with 95% confidence in rotated convention (red) and in (N, E) convention (green), on a PSB were plotted by 'psvelo' module of GMT [67].

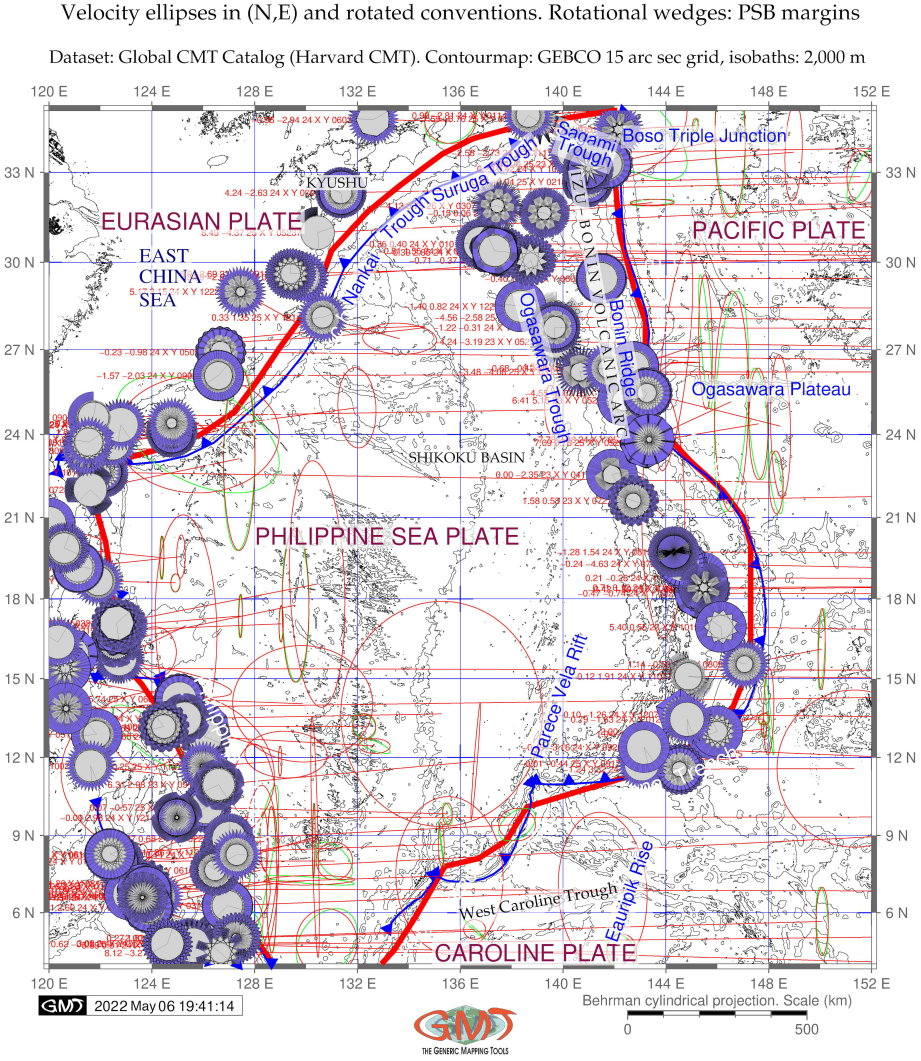

Fig. 6 – (Color online) Velocity ellipses at PSB margins from 1976 to 2010 in (N, E) convention (green) and rotated convention (red). Rotational wedges (purple 'gear wheels'): by 'psvelo' module of GMT. Data: Global CMT Project. Contour: GEBCO grid. Source: author.

The theoretical background of the best-fitting angular velocities and the Mid-

Ocean Ridge VELocity (MORVEL) is presented by [7] who described and modelled geologically current motions of 25 tectonic plates using geologically determined and geodetically constrained subsets of the global circuit. The datasets include the Pacific VELocity (PVEL) [61]. Technical visualisation of the velocity map (Fig. 6) was performed using the following GMT code snippet:

- Velocity ellipses in (N,E) convention: $gmtpsveloCMT.txt - R - J - W0.3p, green - L - Ggreen - Se0.1/0.95/5 - A0.2p - O - K >> ps$. Here, the Vscale gives the scaling of the velocity in inches; the CMT.txt is the dataset; parameters -R and -J indicate the region (here coordinates: -R120/152/4/35)
- Velocity ellipses in rotated convention: $gmtpsveloCMT.txt - R - J - W0.3p, red - Sr0.1/0.95/5 - Ggreen - A0.2p - O - K >> ps$. Here the 'Sr0.1/0.95/5' is the main kwargs showing the Vscale (0.1 inch), Confidence (0.95) and Fontsize (5pt).
- Rotational wedges: $gmtpsveloCMT.txt - R - J - W0.05p - L - Sw0.5/1.e7 - D2 - Gslateblue2 - Elightgray - A0.2p - O - K >> ps$.
  Here, the '-Sw0.5/1.e7' indicates Rotational wedges with kwargs as $Wedge\_scale$ and Wedge_mag. The '-D2' parameter enables to rescale the uncertainties of velocities by
  $sigma\_scale$ (in this case 2 scale was set up).

The respective red and green circles with confidence ellipses are PVEL dataset estimates, which use a plate circuit to estimate subduction across the plate subduction zones in the west Pacific. According to [6], relative to the PSP, the Pacific plate rotates counter-clockwise around a pole near the southern end of the plate boundary. The best-fitting angular velocity indicates rapid decrease of the convergence rates southward, from $49pm0.7mmyr^{-1}(1\sigma)$ at the northern end of the IBM to 9 pm 0.8 mm $yr^{-}1$ of orthogonal subduction along the southern Yap trench, south off Mariana Trench [7].

The PSP-Pacific plate velocities are estimated to fit the interval 1 mm yr-1 and 2° along the lithospheric plate boundary [61], which reflects the overlap in the Global Positioning System (GPS) stations used to estimate the motions of the two plates. The existence of the Caroline plate was first proposed by [65] who estimated its motions from a synthesis of marine seismic, bathymetric, and seismologic observations from its boundaries with the Pacific plates. Located in the western equatorial Pacific immediately south of the PSP (Fig. 1), it remains the poorly understood and one of the most enigmatic tectonic plates with uncertainties about the style and rate of its present deformation caused by the scarcity of reliable kinematic data.

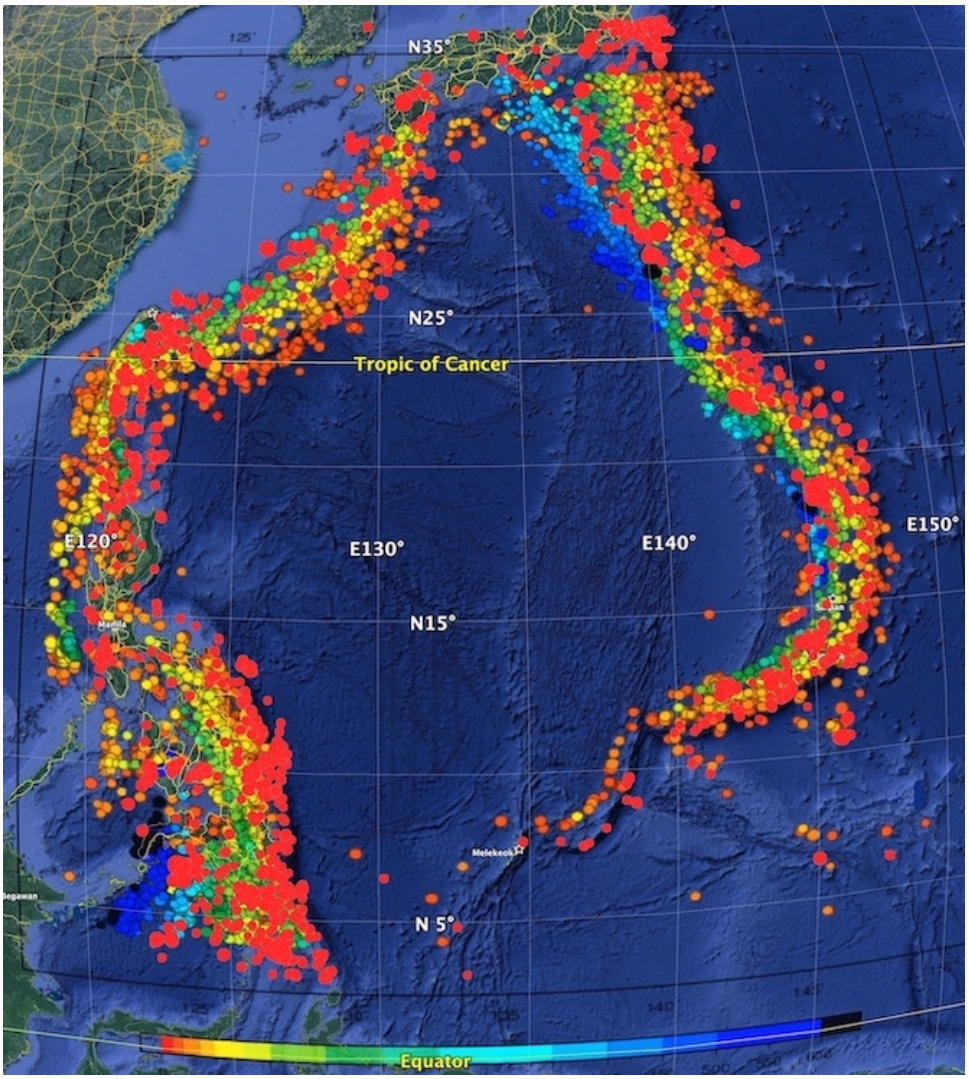

Fig. 7 – (Color online) Earthquakes event map at PSB area: prime hypocentres and magnitude values. Data source: http://www.isc.ac.uk/isc-ehb/search/catalogue/ ISC-EHB Bulletin. Circle size shows a magnitude value. Circle colour shows a hypocenter depth in km (from red: 0 to dark blue/black: > 600). Cartographic overlay of the .kmz data in a format of Keyhole Markup Language: Google Earth Pro. Source: author.

3. RESULTS AND DISCUSSION

Seismic activity is the PSB (Fig. 3) results from the tectonic processes at the edges of the lithospheric plates that spread apart at the ocean ridges along the large

strike-slip faults and converge at the hot and weak volcanic island arcs of the IBM and the Philippines. The seismicity map (Fig. 3) shows that the majority of earthquakes are confined to the marginal areas presenting a narrow, continuous belts around the large stable areas of the PSP. Seismic activity differs by the divergence and convergence zones from moderate in the zones of plate divergence to including deep shocks at shallow depths in the zones of plate convergence. Seismic data on focal mechanisms from the CMT catalogue give a relative direction of the tectonic plates motion throughout the active belts. The focal mechanisms point at the motions of the lithosphere plates determined from the magnetic and topographic data associated with the zones of the plate divergence.

A phenomena of the seismicity in the margins of the lithosphere plates has a tight correlation with the deep-sea trench formation which includes its migration depending primarily on the age of the trench [9, 21]. Thus, located in the place of the subduction plate boundary at a given time, a trench may change its location over time as a result of the complex processes of the global plate tectonics. As proved previously [29], trench migration and related geomorphic fluctuations depend on the lower plate parameters and largely controlled by the subducting plate velocity V_{sub}.

The PSB is marked by the complex interaction of three lithospheric plates: Eurasian, Australian and the PSP, which includes the processes of their collision, subduction and accretion. Old, heavy and large ($103,300,000\,km^2$) Pacific plate plays the major role comparing to the Australian Plate ($47,000,000\,km^2$) and the PSP $5,500,000\,km^2$ [1]. The morphology of the Pacific plate has a low dip angle at shallow depths. The PSP, a large and tectonically complex region of the western Pacific located between the Pacific, Eurasian and Australian plates, is the world's largest marginal basin plate [55]. The PSP has two back-arc basins formed in Oligocene to Miocene period: Parece Vela and Shikoku Basins (Fig. 1).

Slab dynamics is one of the important driving forces for the submarine seismicity and trench formation affecting the mechanisms of its migration (retreat or advance). It is therefore crucial to characterise the origin of the subducting slab morphology in the deep mantle identifying the features of subduction zones, which are among the fundamental issues of solid Earth [70]. Other impacts are caused by the effects of slab mineralogy and phase chemistry on the subduction dynamics (buoyancy, stress field), kinematics (rate of subduction and plate motion), elasticity (deformation and seismic wave speed), thermometry (effects of latent heat, isobaric superheating) and seismicity (adiabatic shear instabilities), as discussed previously [2].

4. CONCLUSION

This paper has extended the practical applications of cartographic scripting and presented a novel series of geophysical maps on PSP for analysis of the seismicity in the western part of the Pacific Ocean. The idea of scripting in cartographic workflow is to model the geospatial datasets by a series of codes written using the GMT syntax and run from a console. Such an approach strengthens the cartographic workflow through automation of tasks and helps avoiding human-induced errors possible by traditional mapping. The presented geophysical maps benefit from the programming principle embedded in the GMT syntax and general coding theory.

The proposed algorithm of the script-based mapping exhibits the advantages that balance the accuracy of cartographic data visualisation and the complexity of geophysical setting in one of the most seismically active regions of the world, – the west Pacific Ocean. Theoretical results on the robustness of geophysical data bound in the presented mapping algorithm are given, and the maps present a complementray sources of information regarding the seismicity in the PSB region. Application of the GMT for geophysical data processing optimises the resulting maps using the method of machine-based plotting through the modular approach of GMT.

The present article introduced a generic cartographic framework for mapping geophysical datasets that were combined with multi-source grids, as explained in detailed in the snippet of codes. The geophysical data included a compilation of GEBCO, ETOPO1, ETOPO5, CMT, EGM96, GVP and Global Self-consistent Hierarchical High-resolution Geography Database (GSHHGD). Also, this study presented an integrated analysis of the seismic and tectonic settings in the PSB. These include visualising the focal mechanisms, velocity and geological lineaments, volcanic activity and general topography of the ocean seafloor in the PSP that are essential for understanding the complex topography of the seabed.

The novelty of this study consists in a script-based data processing for geophysical analysis performed on the PSB. The seismicity data included earthquake locations, magnitude and intensity *via* the GMT modules. Practical novelty of the work consists in the tested methodology of the GMT-based geophysical data visualisation using available techniques [16, 62] as a combination of the geophysical visualisation, geological analysis and GMT-based mapping of the PSB.

In contrast to the state-of-the-art mapping using Graphical User Interface (GUI), *e.g.*, GRASS GIS, SAGA GIS, QGIS [27, 28, 48, 66, 69], or statistical approaches [20, 57], the GMT is notable for scripting algorithms as a core conceptual idea. Thus, compared to the conventional Geographic Information System (GIS), the GMT proposes a more advanced solution on automation through the script-based mapping which results in a high quality mapping [13, 25, 44, 54, 64]. Specifically, among other modules, the 'psmeca', 'psvelo' were tested and demonstrated as useful tools

for geophysical mapping. The semi-automated methods of cartographic data handling is driven by the developed algorithms of console-based scripts [59]. The use of scripts in a cartographic workflow minimises handmade routine and subjectivity and increases the overall precision and accuracy of mapping.

Rigorous evaluation of the open source GIS data on the southern side of the PSB showed that current geophysical situation is largely affected by the geologic evolution of the PSB. Technically, the performed mapping by GMT showed that the scripting cartographic algorithms outperform the state-of-the-art GIS software in terms of data processing and handling. This is achieved *via* the use of scripts that have a high accuracy of plotting. Besides, scripts may be reused as templates, modified and optimised for similar studies on the geophysics of the Pacific Ocean. This increases the value of programming in a cartographic workflow for future studies.

5. ACRONYMS AND ABBREVIATIONS

ASCII American Standard Code for Information Interchange

CMT Centroid Moment Tensor

EGM96 Earth Gravitational Model 1996

EHB Engdahl-van der Hilst-Buland algorithm

GEBCO General Bathymetric Chart of the Oceans

GIS Geographic Information System

GMT Generic Mapping Tools

GPS Global Positioning System

GSHHGD Global Self-consistent Hierarchical High-resolution Geography Database

GUI Graphical User Interface

IBM Izu-Bonin-Mariana trench

ISC International Seismological Centre

KMZ Keyhole Markup language Zipped

KPR Kyushu-Palau Ridge

Mb Body wave magnitude

MORVEL Mid-Ocean Ridge VELocity

Ms Surface wave magnitude

Mw Moment magnitude

PSB Philippine Sea Basin

PSP Philippine Sea Plate

PVEL Pacific VELocity

RS Richter Scale

WGS84 World Geodetic System 1984

REFERENCES

1. A. Alden, Here are the Sizes of Tectonic or Lithospheric Plates (2019). Retrieved from https://www.thoughtco.com/sizes-of-tectonic-or-lithospheric-plates-4090143
2. C.R. Bina, S. Stein, F.C. Marton, E.M. Van Ark, *Implications of slab mineralogy for subduction dynamics*. Phys. Earth Planet. Inter. **127**, 51–66 (2001). doi: 10.1016/S0031-9201(01)00221-7
3. L. Cao, Z. Wang, S. Wu, X. Gao, *A new model of slab tear of the subducting Philippine Sea Plate associated with Kyushu-Palau Ridge subduction*. Tectonophysics **636**, 158–169 (2014). doi: 10.1016/j.tecto.2014.08.012
4. W.Y. Chang, G.K. Yu, R.D. Hwang, J.K. Chiu, *Lateral Variations of Rayleigh-wave Dispersions in the Philippine Sea region*. Terr. Atmospheric Ocean. Sci. **18**, 859–878 (2007). doi: 10.3319/TAO.2007.18.5.859(T)
5. H. Cížková, C.R. Bina, *Geodynamics of trench advance: Insights from a Philippine-Sea-style geometry*. Earth Planet. Sci. Lett. E. **430**, 408–415 (2015). doi: 10.1016/j.epsl.2015.07.004
6. C. DeMets, R.G. Gordon, D.F. Argus, S. Stein, *Current plate motions*. Geophys. J. Int. **101**, 425–478 (1990). doi: 10.1111/j.1365-246X.1990.tb06579.x
7. C. DeMets, R.G. Gordon, D.F. Argus, *Geologically current plate motions*. Geophys. J. Int. **181**, 1–80 (2010). doi: 10.1111/j.1365-246X.2009.04491.x
8. G. Ekström, M. Nettles, A.M. Dziewonski, *The global CMT project 2004-2010: Centroid-moment tensors for 13,017 earthquakes*. Phys. Earth Planet. Inter. **200–201**, 1–9 (2012). doi: 10.1016/j.pepi.2012.04.002
9. C. Faccenna, E.D. Giuseppe, F. Funiciello, S. Lallemand, J. van Hunen, *Control of seafloor aging on the migration of the Izu-Bonin-Mariana Trench*. Earth Planet. Sci. Lett. **288**, 386–398 (2009). doi: 10.1016/j.epsl.2009.09.042
10. P. Lemenkova, *Console-Based Mapping of Mongolia Using GMT Cartographic Scripting Toolset for Processing TerraClimate Data*. Geosciences, **12**(3), 140 (2022). doi: 10.3390/geosciences12030140
11. M.N. Hill, *Recent geophysical exploration of the ocean floor*. Phys. Chem. Earth **2**, 129–163 (1957). doi: 10.1016/0079-1946(57)90008-3.
12. Y. Tang, D. Cao, *A preliminary study on present tectonic stress field in the southeast part of North China and its vicinity*. Phys. Chem. Earth **17**, 219–226 (1990). doi: 10.1016/0079-1946(89)90028-1.
13. P. Lemenkova, *Using GMT for 2D and 3D Modeling of the Ryukyu Trench Topography, Pacific Ocean*. Misc. Geogr. **25**(3), 1–13 (2020). doi: 10.2478/mgrsd-2020-0038
14. K. Fujioka, K. Okino, T. Kanamatsu, Y. Ohara, O. Ishizuka, S. Haraguchi, T. Ishii, *Enigmatic extinct spreading center in the West Philippine backarc basin unveiled*. Geology **27**, 1135–1138 (1999). doi: 10.1130/0091-7613(1999)027¡1135:EESCIT¿2.3.CO;2
15. K. Fujioka, K. Okino, T. Kanamatsu, Y. Ohara, *Morphology and origin of the Challenger Deep in the Southern Mariana Trench*. Geophys. Res. Lett. **29**, 13–72 (2002). doi: 10.1029/2001GL013595
16. P. Lemenkova, *Tanzania Craton, Serengeti Plain and Eastern Rift Valley: mapping of geospatial data by scripting techniques*. Estonian J. Earth Sci. **71(2)**, 61–79 (2022). doi: 10.3176/earth.2022.05
17. W. Gong, X. Jiang, Y. Guo, J. Xing, C. Li, Y. Sun, *Strike-slip tectonics within the northernmost Philippine Sea plate in an arc continent collisional setting*. J. Asian Earth Sci. **146**, 265–278 (2017). doi: 10.1016/j.jseaes.2017.05.032
18. I.S. Sacks, J.A. Snoke, *Seismological determinations of the subcrustal continental lithosphere*. Phys. Chem. Earth **15**, 3–37 (1984). doi: 10.1016/0079-1946(84)90003-X.
19. Q. Di, F. Tian, Y. Suo, R. Gao, S. Li, C. Fu, G. Wang, F. Li, Y. Tan, *Linkage of deep*

lithospheric structures to intraplate earthquakes: A perspective from multi-source and multi-scale geophysical data in the South China Block. Earth-Sci. Rev. **214**, 103504 (2021). doi: 10.1016/j.earscirev.2021.103504.

20. P. Lemenkova, *Testing Linear Regressions by StatsModel Library of Python for Oceanological Data Interpretation*. Aquatic Sciences and Engineering **34**(2), 51–60 (2019). doi: 10.26650/ASE2019547010
21. M.A. Gutscher, F. Klingelhoefer, T. Theunissen, W. Spakman, T. Berthet, T.K. Wang, C.S. Lee, *Thermal modeling of the SW Ryukyu forearc (Taiwan): Implications for the seismogenic zone and the age of the subducting Philippine Sea Plate (Huatung Basin)*. Tectonophysics **692**, 131–142 (2016). doi: 10.1016/j.tecto.2016.03.029
22. P. Lemenkova, *NOAA Marine Geophysical Data and a GEBCO Grid for the Topographical Analysis of Japanese Archipelago by Means of GRASS GIS and GDAL Library*. Geomat. Environ. Eng. **14**(4), 25–45 (2020). doi: 10.7494/geom.2020.14.4.25
23. R. Hall, J.R. Ali, C.D. Anderson, S.J. Baker, *Origin and motion history of the Philippine Sea Plate*. Tectonophysics **251**, 229–250 (1995). doi: 10.1016/0040-1951(95)00038-0
24. R. Hall, M. Fuller, J.R. Ali, C.D. Anderson, *The Philippine Sea Plate: magnetism and reconstructions*. Geophys. Monogr. Ser. AGU, Active Margins and Marginal Basins of the Western Pacific **88**, 371–404 (1995). doi: 10.1029/GM088p0371
25. P. Lemenkova, *Variations in the bathymetry and bottom morphology of the Izu-Bonin Trench modelled by GMT*. Bull. Geogr. Phys. Geogr. Ser. **18**(1), 41–60 (2020). doi: 10.2478/bgeo-2020-0004
26. J. Barretto, R. Wood, J. Milsom, *Benham Rise unveiled: Morphology and structure of an Eocene large igneous province in the West Philippine Basin*. Mar. Geol. **419**, 106052 (2020). doi: 10.1016/j.margeo.2019.106052
27. M. Klaučo, B. Gregorová, U. Stankov, V. Marković, P. Lemenkova, *Land planning as a support for sustainable development based on tourism: A case study of Slovak Rural Region*. Environ. Eng. Manag. J. **2**(16), 449–458 (2017). doi: 10.30638/eemj.2017.045
28. M. Klaučo, B. Gregorová, U. Stankov, V. Marković, P. Lemenkova, *Determination of ecological significance based on geostatistical assessment: a case study from the Slovak Natura 2000 protected area*. Open Geosci. **5**(1), 28–42 (2013). doi: 10.2478/s13533-012-0120-0
29. S. Lallemand, A. Heuret, C. Faccenna, F. Funiciello, *Subduction dynamics as revealed by trench migration*. Tectonics **27**, TC3014 (2008). doi: 10.1029/2007TC002212
30. J.Y. Lin, C.L. Lo, *Earthquake-induced crustal gravitational potential energy change in the Philippine area*. J. Asian Earth Sci. **66**, 215–223 (2013). doi: 10.1016/j.jseaes.2013.01.009
31. H.W. Menard, *Deep-sea channels, topography, and sedimentation*. Am. Assoc. Pet. Geol. Bull. **39**, 236–255 (1955).
32. P. Lemenkova, *Mapping topographic, geophysical and gravimetry data of Pakistan - a contribution to geological understanding of Sulaiman Fold Belt and Muslim Bagh Ophiolite Complex*. Geophysica **56**(1–2), 3–26 (2021). doi: 10.5281/zenodo.5779189
33. D. Müller, *Deep Earth Structure and Global Tectonics*. University of Sydney, School of Geosciences, Division of Geology and Geophysics, GEOL Geological Hazards and Solutions (2001).
34. Y. Ogawa, K. Kobayashi, H. Hotta, K. Fujioka, *Tension cracks on the oceanward slopes of the northern Japan and Mariana Trenches*. Mar. Geol. **141**, 111–123 (1997). doi: 10.1016/S0025-3227(97)00059-5
35. P. Lemenkova, *GMT Based Comparative Analysis and Geomorphological Mapping of the Kermadec and Tonga Trenches, Southwest Pacific Ocean*. Geogr. Tech. **14**(2), 39–48 (2019). doi: 10.21163/GT_2019.142.04
36. N. Uchida, T. Matsuzawa, J. Nakajima, A. Hasegawa, *Subduction of a wedge-shaped Philippine*

Sea plate beneath Kanto, central Japan, estimated from converted waves and small repeating earthquakes, J. Geophys. Res. Solid Earth **115**(B7) (2010). doi: 10.1029/2009JB006962

37. Z. Ma, *Seismic data attribute extraction based on Hadoop platform*, 2017 IEEE 2nd Intl. Conf. Cloud Computing and Big Data Analysis (ICCCBDA), 180–184 (2017). doi: 10.1109/ICCCBDA.2017.7951907
38. P. Lemenkova, *Statistical Analysis of the Mariana Trench Geomorphology Using R Programming Language*. Geod. Cartogr. **45**(2), 57–84 (2019). doi: 10.3846/gac.2019.3785
39. A. Ozawa, T. Tagami, E.L. Listanco, C.B. Arpa, M. Sudo, *Initiation and propagation of subduction along the Philippine Trench: evidence from the temporal and spatial distribution of volcanoes*. J. Asian Earth Sci. **23**, 105–111 (2004). doi: 10.1016/S1367-9120(03)00112-3
40. N.K. Pavlis, S.A. Holmes, S.C. Kenyon, J.K. Factor, *The development and evaluation of the Earth Gravitational Model 2008 (EGM2008)*. J. Geophys. Res. **117**, B04406 (2012). doi: 10.1029/2011JB008916
41. P. Lemenkova, *Submarine tectonic geomorphology of the Pliny and Hellenic Trenches reflecting geologic evolution of the southern Greece*. Rud. Geolosko Naft. Zb. **36**(4), 33–48 (2021). doi: 10.17794/rgn.2021.4.4
42. M. Zhang, P. Yue, X. Guo, *GIScript: Towards an interoperable geospatial scripting language for GIS programming*. 2014 The Third Intl. Conf. Agro-Geoinformatics (2014), 1–5. doi: 10.1109/Agro-Geoinformatics.2014.6910592
43. I.R. Samowitz, D.W. Forsyth, *Double seismic zone beneath the Mariana Island arc*. J. Geophys. Res. **86**, 7013–7021 (1981). doi: 10.1029/JB086iB08p07013
44. P. Lemenkova, *Java and Sumatra Segments of the Sunda Trench: Geomorphology and Geophysical Settings Analysed and Visualized by GMT*. Glasnik Srpskog Geografskog Drustva, **100**(2), 1–23 (2020). doi: 10.2298/GSGD2002001L
45. H. Kimura, K. Kasahara, T. Takeda, *Subduction process of the Philippine Sea Plate off the Kanto district, central Japan, as revealed by plate structure and repeating earthquakes*. Tectonophysics **472**(1), 18–27 (2009). doi: 10.1016/j.tecto.2008.05.012.
46. N.E. Parcutela, C.B. Dimalanta, L.T. Armada, G.P. Yumul, *PHILCRUST3.0: New constraints in crustal growth rate computations for the Philippine arc*. J. Asian Earth Sci.: X. **4**, 100032 (2020). doi: 10.1016/j.jaesx.2020.100032
47. K. Suzuki, M. Nakano, N. Takahashi, T. Hori, S. Kamiya, E. Araki, R. Nakata, Y. Kaneda, *Synchronous changes in the seismicity rate and ocean-bottom hydrostatic pressures along the Nankai trough: A possible slow slip event detected by the Dense Oceanfloor Network system for Earthquakes and Tsunamis (DONET)*. Tectonophysics **680**, 90–98 (2016). 10.1016/j.tecto.2016.05.012.
48. P. Lemenkova, *Dataset compilation by GRASS GIS for thematic mapping of Antarctica: Topographic surface, ice thickness, subglacial bed elevation and sediment thickness*. Czech Polar Rep. **11**(1), 67–85 (2021). doi: 10.5817/CPR2021-1-6
49. X. Bu, P. Yue, L. Wang, M. Zhang. *A scripting approach for integrating software packages and geoprocessing services into scientific workflows*. 2015 Fourth Intl. Conf. Agro-Geoinformatics (Agro-geoinformatics), 15–18 (2015). doi: 10.1109/Agro-Geoinformatics.2015.7248095
50. S. Bhattacharjee, L.B.A. Rahim. *A Hadoop Allied Security Platform for Seismic Big Data Processing*. 2021 Intl. Conf. Computer Information Sciences (ICCOINS) 372–377 (2021). doi: 10.1109/ICCOINS49721.2021.9497221
51. P. Lemenkova, *Topography of the Aleutian Trench south-east off Bowers Ridge, Bering Sea, in the context of the geological development of North Pacific Ocean*. Baltica **34**(1), 27–46 (2021). doi: 10.5200/baltica.2021.1.3
52. Q. Zu, C.-H. Chen, C.-R. Chen, S. Liu, H.-Y. Yen, *The relationship among earthquake location,*

magnetization, and subsurface temperature beneath the Taiwan areas. Phys. Earth Planet. Inter. **320**, 106800 (2021). doi: 10.1016/j.pepi.2021.106800.

53. T. Saito, T. Baba, D. Inazu, S. Takemura, E. Fukuyama, *Synthesizing sea surface height change including seismic waves and tsunami using a dynamic rupture scenario of anticipated Nankai trough earthquakes*. Tectonophysics **769**, 228166 (2019). doi: 10.1016/j.tecto.2019.228166.
54. P. Lemenkova, *Geomorphology of the Puerto Rico Trench and Cayman Trough in the Context of the Geological Evolution of the Caribbean Sea*. Ann. Univ. Mariae Curie-Skłodowska, B Geogr. Geol. Mineral. Petrogr. **75**, 115–141 (2020). doi: 10.17951/b.2020.75.115-141
55. M. Sdrolias, W.R. Roest, R.D. Müller, *An expression of Philippine Sea plate rotation: the Parece Vela and Shikoku Basins*. Tectonophysics **394**, 69–86 (2004). doi: 10.1016/j.tecto.2004.07.061
56. Y. Yan, L. Huang, L. Yi, *Is Apache Spark scalable to seismic data analytics and computations?* 2015 IEEE Intl. Conf. Big Data (Big Data), 2036–2045 (2015). doi: 10.1109/BigData.2015.7363985
57. P. Lemenkova, *AWK and GNU Octave Programming Languages Integrated with Generic Mapping Tools for Geomorphological Analysis*. GeoSci. Eng. **65**(4), 1–22 (2019). doi: 10.35180/gse-2019-0020
58. B. Li, Y. Li, W. Jiang, Z. Su, W. Shen, *Conjugate ruptures and seismotectonic implications of the 2019 Mindanao earthquake sequence inferred from Sentinel-1 InSAR data*. Int. J. Appl. Earth Obs. Geoinf. **90**, 102127 (2020). doi: 10.1016/j.jag.2020.102127.
59. P. Lemenkova, *Robust Vegetation Detection Using RGB Colour Composites and Isoclust Classification of the Landsat TM Image*. Geomatics, Landmanagement and Landscape **4**, 147–167 (2021). doi: 10.5281/zenodo.6347500
60. L.C. Seekings, T.L. Teng, *Lateral variations in the structure of the Philippine Sea Plate*. J. Geophys. Res. **82**, 317–324 (1977). doi: 10.1029/JB082i002p00317
61. G.F. Sella, T.H. Dixon, A. Mao, *REVEL: a model for recent plate velocities from space geodesy*. J. Geophys. Res. **107**, 11–30 (2002). doi: 10.1029/2000JB000033
62. P. Lemenkova, *Seismicity in the Afar Depression and Great Rift Valley, Ethiopia*. Environ. Res. Eng. Manag. **78**(1), 83–96 (2022). doi: 10.5755/j01.erem.78.1.29963
63. S. Hori, *Seismic activity associated with the subducting motion of the Philippine Sea plate beneath the Kanto district, Japan*. Tectonophysics **417**(1), 85–100 (2006). doi: 10.1016/j.tecto.2005.08.027
64. P. Lemenkova, *GEBCO Gridded Bathymetric Datasets for Mapping Japan Trench Geomorphology by Means of GMT Scripting Toolset*. Geod. Cartogr. **46**(3), 98–112 (2020). doi: 10.3846/gac.2020.11524
65. J.K. Weissel, R.N. Anderson, *Is there a Caroline plate?* Earth Planet. Sci. Lett. **41**, 143–158 (1978). doi: 10.1016/0012-821X(78)90004-3
66. P. Lemenkova, *Sentinel-2 for High Resolution Mapping of Slope-Based Vegetation Indices Using Machine Learning by SAGA GIS*. Transylv. Rev. Syst. Ecol. Res. **22**(3), 17–34 (2020). doi: 10.2478/trser-2020-0015
67. P. Wessel, W.H.F. Smith, *New, improved version of generic mapping tools released*. EOS Trans. AGU **79**(47), 579–579 (1998). doi: 10.1029/98EO00426
68. T. Iidaka, T. Igarashi, A. Hashima, A. Kato, T. Iwasaki, *Receiver function images of the distorted Philippine Sea slab contact with the continental crust: Implications for generation of the 1891 Nobi earthquake (Mj 8.0)*. Tectonophysics **717**, 41–50 (2017). doi: 10.1016/j.tecto.2017.07.010
69. P. Lemenkova, *Geophysical Mapping of Ghana Using Advanced Cartographic Tool GMT*. Kartogr. i Geoinformacije **20**(36), 16–37 (2021). doi: 10.32909/kg.20.36.2

70. M. Yoshida, *Trench dynamics: Effects of dynamically migrating trench on subducting slab morphology and characteristics of subduction zones systems*. Phys. Earth Planet. Inter. **268**, 35–53 (2017). doi: 10.1016/j.pepi.2017.05.004